A Collision Risk Assessment Method for Runway Threshold Management: A Case Study of Singapore Changi Airport

Haojie Ang[a], Qing Cai[a], Sameer Alam[a,*]

[a] *Air Traffic Management Research Institute, School of Mechanical and Aerospace Engineering, Nanyang Technological University, Singapore, 639798*

Abstract

Airports are indispensable infrastructures in an air transportation system with runways being the most critical component serving departures and arrivals. With constant increase in demand of air traffic, much effort has been made to manage the runway capacity to improve the throughput of airports. Apart from operational changes, there is a significant investment in runway infrastructure improvements such as new runway development/extension. However, many runways suffer from long runway thresholds due to safety constraints in face of approach path obstacles, which leads to reduction in Landing Distance Available (LDA), thereby reducing runway capacity. This paper proposes a method to manage the runway threshold by computing and assessing the collision risk of a given flight approach path with an obstacle profile. To do so, we develop the arrival flight profile along with the altitude distribution the landing aircraft using ADS-B data. We then factor in the height of obstacles with reference to the obstacle surface profile. The convolution of two distribution is then used to assess the collision risk between the aircraft on approach path and the obstacle for better management of runway threshold. The proposed model is applied to Singapore Changi Airport, which has a long runway threshold due to the ship movements in the Strait of Singapore, which are considered as safety risks to the landing aircraft. Results suggest that, for CAT I/II approaches, with aircraft having aerodrome reference code 3/4, the runway threshold for runway Singapore Changi Airport 20R can safely be reduced by approximately 100 meters, while meeting the safety requirements. This increases the Landing Distance available and may lead to an increase runway capacity.

Keywords: Air traffic management, system safety, collision risk, runway threshold management, Singapore Changi International Airport

1. Introduction

Air traffic plays an important role in the growing economy of the world [1–3]. According to International Air Transport Association (IATA), the amount of passengers is predicted to hit 8.2 billion by the year 2037 based on the present trend [4]. With the continuous increase in air traffic demand, congestion at airports is inevitable [5, 6] which contributes to the safety risks of air traffic [7, 8]. Therefore, airports have to come out with new plans to mitigate air traffic congestion [9–11] so as to ensure the system safety of air traffic [12]. Note that runways are among the most critical components in effecting airport capacity [13]. Therefore, in order to accommodate more air traffic, one of the most effective ways is efficient management of runways [14].

Tremendous effort has been made towards efficient runway management. Existing endeavours can be roughly categorised into two classes, viz., runway operational/procedural improvements [15, 16] and runway infrastructure improvements. From the operational/procedural perspective, research such as Runway Configuration Management (RCM), Arrival Departure Runway Balancing (ADRB) [17–19], Runway Occupancy Time management [20], System Oriented Runway Management (SORM) [21], etc., have been developed to improve the runway management for airports [13, 22–24]. However, there is limited improvement that these approaches can bring about due to complex interactions of several sub-systems in air traffic management which limits the full realization of such effort. Compared to operational and procedural improvements, runway infrastructure improvements such as extending existing runways and building new ones could be more

*Corresponding author
Email address: sameeralam@ntu.edu.sg (Sameer Alam)

straightforward [25] and effective to cope with air traffic demand. However, there are many factors which are required to be considered before proceeding. For example, building a new runway has to take into account the cost, noise effect, local environmental concerns, etc., while extending a runway may subject to limited land availability and safety concerns (converging runways, availability of Stop-Way, Clearway and Runway Safety Area, etc.) [26].

Due to the limited space of cities and also to reduce the noise effect of the aircraft that can cause disturbance to the city residents, many airports/runways such as Kansai International Airport, Hong Kong International Airport, Incheon International Airport, Singapore Changi Airport etc., are built on reclaimed land [27, 28]. One of the major safety risks for those runways is the movements of ships in the sea which can interfere in the approach path of arrivals. In order to maintain the safety standard, a displaced threshold is stipulated to the runways to avoid collision between the arrival flights and the ship. However, most of those runway thresholds were developed in a conservative manner leading to a runway threshold that takes away a considerable runway length. For example, the runway threshold for Macau International Airport is 364m and Singapore Changi International Airport is 740m. If the threshold of a runway can be managed (reduced) the Landing Distance Available (LDA) can be increased, and as a consequence, the runway capacity may be increased due to increased availability of runway exits (previously inaccessible), wide-body aircraft operations (which may require longer LDA), and runway safety (reducing the chances of runway excursions) [29, 30]. Thus, there is a window of opportunity for several such airports (build on reclaimed land on sea) in the world, to manage the runway thresholds efficiently, in order to improve capacity and safety.

This work aims to manage the runway threshold in order to increase the LDA. To do so, we propose a data-driven method and a computational model to reduce the runway threshold by making use of the flight trajectory data and the obstruction surface profile as per the ICAO standards on Approach Surface Obstacles [31]. The proposed model allows for flight path obstruction analysis leading to reduction in runway threshold distance. To validate the effectiveness of the proposed method, we carry out a case study on Singapore Changi International Airport, hereafter termed as Changi Airport. Changi Airport, being one of the major air transport hub in Southeastern Asia, had handled over 380,000 aircraft movements in 2018 and may also face traffic congestion in the future due to the increasing air traffic demand [32]. Changi Airport is one of the airports that is built on a reclaimed land and is situated at the eastern end of Singapore which is surrounded by the Singapore Strait [33]. Fig. 1 shows the runway 20R, which is of interest, and the surrounding Singapore Strait. Due to the ship movements in the Singapore Strait, a permanently displaced threshold is provided for runway 20R.

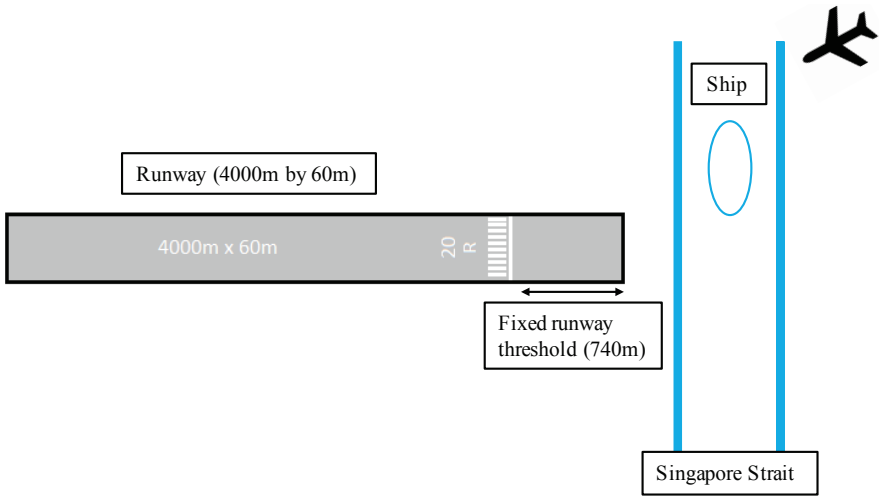

Figure 1: Graphical illustration of runway 20R and the surrounding Singapore Strait. The ship movements in Singapore Strait result in a permanently displaced threshold of 740m.

Due to the unique geographical location of Singapore, ship movements in the Singapore Strait are considered as an obstruction to surrounding airspace due to the height of the ship [34]. As runway 20R has a heading facing the Singapore Strait, a permanently displaced threshold of 740m is regulated for that runway [35]. This is determined by imposing a highly conservative maximum safety limit based on the height

of ship, that passes through the Singapore Strait. However, this conservative set up may result in a loss of runway length (LDA) which leads to lower runway capacity.

With the increased availability of ADS-B data in approach and landing phase, we now have a better insight into aircraft landing profile. Further the ship movement data in Singapore Strait along with the tidal waves data which is available from Meteorological Service Singapore and Windfinder, can allow us to better model the approach obstructions profile such that the runway threshold can be better managed.

The remainder of this paper is organized as follows. Section 2 illustrates the research background that is required to understand the research problem intended to address. Section 3 describes the research methodology and the developed method for runway threshold management. Section 4 presents the experimental settings for the application of our proposed method to Changi Airport while section 5 demonstrates the experimental results. Concluding remarks are then provided in Section 6.

2. Research Backgrounds

2.1. Obstacle Limitation Surfaces

Obstacles surrounding the aerodrome impact the aircraft landing and take-off and are the main factors for determining the runway threshold configuration. In this section we introduce the concept of obstacle limitation surfaces around the runway based upon the ICAO Annex 14 Aerodromes (Obstacle Restriction and Removal), hereafter referred to as Annex-14.

An aerodrome is a defined area on land or sea where flight operations take place. Annex-14 defines the airspace around the aerodromes to be kept free from obstacles to allow the usual operations of aircraft to operate safely and to eliminate the chance that aerodromes become unusable due to the construction of obstacles around the aerodromes. Therefore, different types of obstacle limitation surfaces (OLS) and their respective limits are established to which an object may extend into the airspace. There are 9 different surfaces namely outer-horizontal surface, conical surface, inner-horizontal surface, approach surface, inner-approach surface, transitional surface, inner-transitional surface, balked-landing surface and take-off climb surface [31]. Fig. 2 illustrates the different types of OLS around the runway. These are imaginary surfaces which must not be violated by any obstacle.

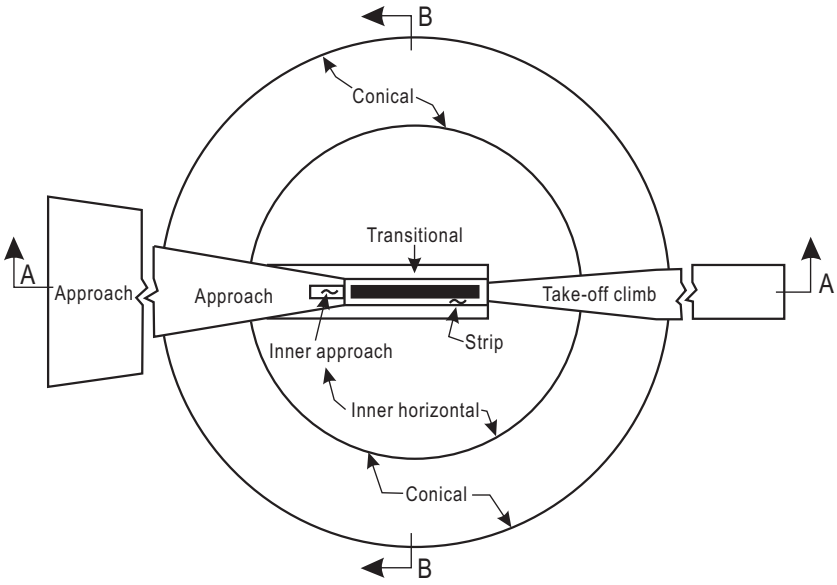

Figure 2: An illustration of different types of obstacle limitation surfaces around the runway [31].

The dimensions of OLS are specified based on different types of approach runways classification and the aircraft aerodrome reference code number. The different classification of approach runways is non-instrument, non-precision approach and precision approach. The aircraft reference code number is classified based on its highest value of the aeroplane reference field length for which the runway is intended [31]. In this work, we are assuming the aircraft is wide-body of code number 3/4 performing a landing approach on the precision

Table 1: Dimension of approach surface based on Precision Approach Category and Aerodrome Reference Code number [31].

Precision Approach Category	Code Element 1		Approach	
	Code Number	Aeroplane reference field length (m)	Distance from threshold (m)	Slope
I	1	(0, 800)	60	2.5%
I	2	[800, 1 200)	60	2.5%
I/II/III	3	[1 200, 1 800)	60	2%
I/II/III	4	[1 800, $+\infty$)	60	2%

approach CAT I/II runway. Table 1 shows the dimension and slopes of the approach surface based on the aerodrome reference code of aircraft and the precision approach CAT I/II runway.

2.2. Approach Surface

In this paper, we are assuming the runway is under precision approach CAT I/II, where the approach surface is an inclined plane or combination of planes directly after the runway threshold. The inner approach surface is a rectangular portion of the approach surfaces directly after the runway threshold. Fig. 3(a) shows the runway threshold, inner approach and approach surface and Fig. 3(b) displays the runway threshold, inner approach and approach surface of runway 20R which is directly after the runway threshold.

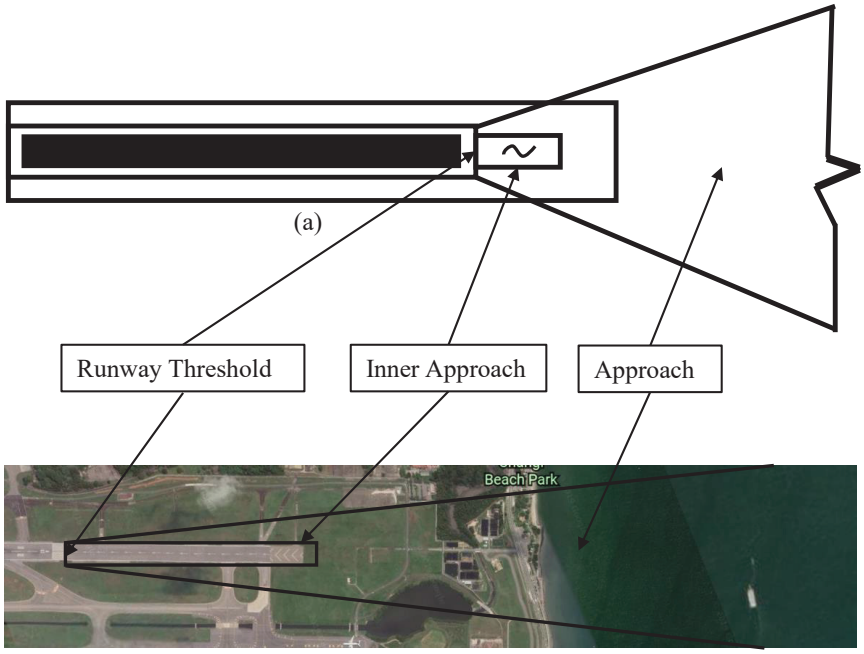

Figure 3: Graphical illustrations of (a) The runway threshold, the inner approach, approach obstacles limitation surfaces and (b) The runway threshold, the inner approach, approach obstacles limitation surface of runway 20R at Changi airport which is obtained from Google Map.

2.3. Displaced Runway Threshold and Landing Distance Available

A displaced runway threshold is a threshold located at a point on the runway other than the designated beginning of the runway. The portion of the runway that is behind the displace threshold can only be used for taxi/takeoff on both direction and landing on opposite direction [36]. Aircraft that is landing on the runway with a displaced runway threshold can only land beyond the displaced threshold marking. The Landing Distance Available (LDA) is defined as the length of runway declared available and is suitable for the landing of aircraft. The LDA may be less than the actual length of the runway or the length of the

runway directly after a displaced threshold not including the Stop-Way and Clearway. Fig. 4 illustrates the displaced threshold markings and the LDA of a runway. Fig. 4(a) illustrates the most common type of runway threshold do not have a displacement and its LDA. Fig. 4(b) illustrates the runway with a displaced threshold and its LDA.

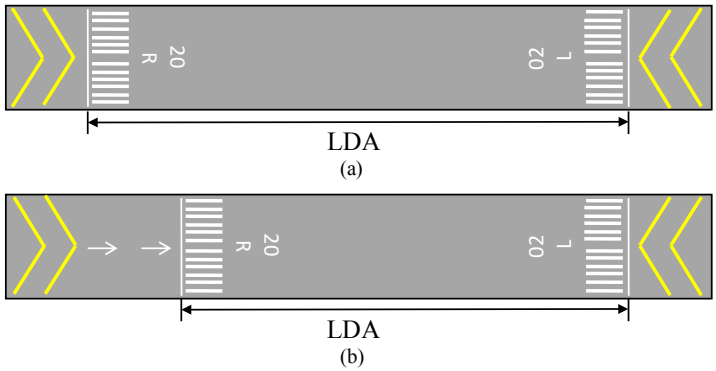

Figure 4: Graphical illustrations of runway markings. (a) Runway threshold that do not have displacement and its LDA, (b) Displaced threshold and its LDA.

3. Problem Description and Methodology

3.1. Problem Description

This work aims to reduce the length of the displaced threshold of a runway after accounting for the obstruction surface profile. Without loss of generality, throughout the paper we consider airports that are build on the reclaimed land over the ocean where ship movement is frequent. Consequently, we consider such ship movements as the obstructions to the aerodrome approach segment.

Currently, the runway of such airports has a displaced threshold to prevent the collision of the aircraft with the ships in the strait during landing. However, the displaced threshold may be a very conservative due to the ximum safety he idea of redı

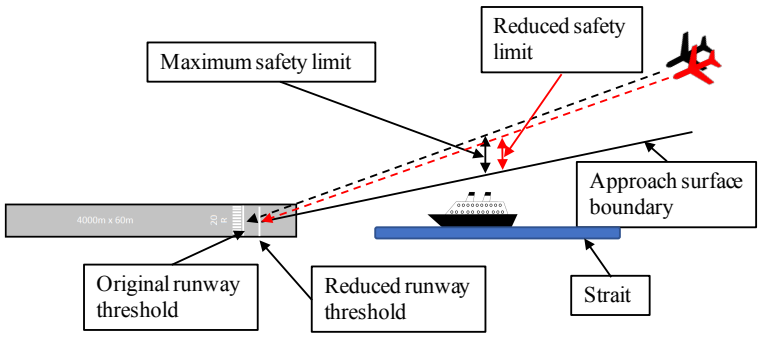

Figure 5: The idea of reducing runway threshold length by reducing the maximum safety limit.

To determine acceptable safety limit, the collision risk between the aircraft and ships must be computed. The crucial data which are required to determine the collision risk is the variations in the height of the ship (due to tidal waves) and the vertical deviations of the aircraft landing trajectory.

3.2. Methodology

Fig. 6 presents a graphical overview of the proposed method. It can be seen from Fig. 6 that the proposed method involves three phases, i.e., the preliminary phase, the developing phase and the experimental phase. In the preliminary phase, the maximum height of the approach surface, maximum height of the ship and

the landing trajectory of the aircraft are being determined. Next, during the developing phase, the normal distribution of the ship's height and the aircraft's altitude is derived and the collision risk between the ship and aircraft is further determined. Finally, in the experimental phase, the collision risk calculation method is applied individually to different shipping lanes to obtain their corresponding collision risk. By analysing the collision risk of the critical lane, the length of runway threshold that can be reduced is estimated.

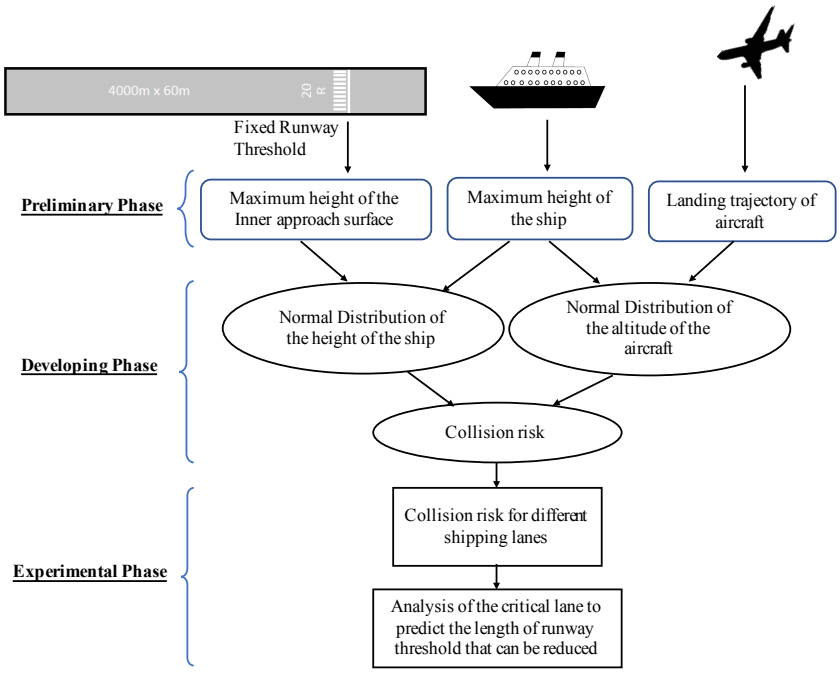

Figure 6: An overview of the proposed method for reducing the runway threshold.

3.3. Research Assumptions and Reasons

In order to solve the research problem given in the above subsection, the following assumptions together with their corresponding reasons are provided.

1) One of the fundamental assumption in the current work is that there is a maximum safety distance limit (see Fig. 5) between the ship and the aircraft. This assumption is made to determine the collision risk in a safer approach.

2) The mean height of the ship is assumed to be maximum height of the approach surface and it can be generated to a normal distribution after accounting for the height of the tidal waves. This assumption is made due to the fact that the height of the ship cannot be above an approach surface as state in the Annex-14.

3) The variations of the height of the ship and the altitude of the aircraft from the landing trajectory are assumed to follow normal distributions. On one hand, Gaussian distribution has very good mathematical properties. On the other hand, the occurrences of many natural phenomena are reported to obey Gaussian distributions.

4) The standard deviation of the altitude of the aircraft at a certain latitude is assumed to remain unchanged when the runway threshold in reduced. This assumption is made as the standard deviation data for lower altitude is not available at the same latitude.

4. Experimental Design

In this paper, we are using Changi Airport as a case study to estimate the length of runway threshold that can be reduced by accounting the collision risk between the aircraft and the ships in Singapore Strait.

Runway 20R is the only runway in Singapore that has a displaced threshold due ship movements in the Singapore Strait. Therefore, the ships in the Singapore strait are considered as the obstruction for the approach aircraft and a displaced threshold is required to clear the obstruction. In this section, the detailed experimental design is presented.

4.1. Runway 20R of Changi Airport and Singapore Strait

The Singapore Strait consists of 3 shipping lanes that facilitate ship movements. The runway threshold of runway 20R is determined by the maximum height limit of the ship in the Singapore Strait. Fig. 7 shows the runway threshold of runway 20R and the lanes in Singapore Strait. The table on the bottom right of Fig. 7 shows the latitude of the starting/middle point of each shipping lane together with its distance to the threshold of the runway.

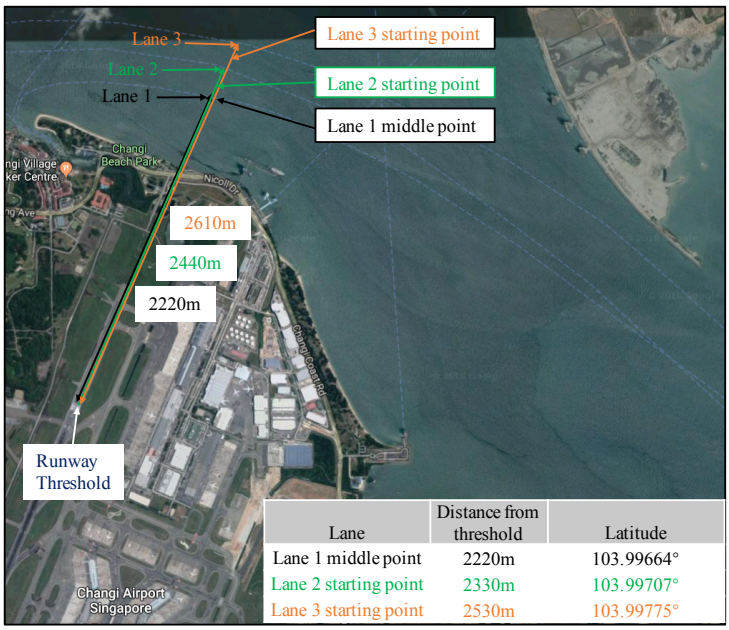

Lane	Distance from threshold	Latitude
Lane 1 middle point	2220m	103.99664°
Lane 2 starting point	2330m	103.99707°
Lane 3 starting point	2530m	103.99775°

Figure 7: Distance from the runway threshold and their corresponding latitude at the starting point of each lane. The picture and the corresponding data are from Google Map.

4.2. Normal Distribution of the Height of the Ship

To generate the normal distribution of the height of the ship, the maximum height of the approach surface which is assumed to be the mean height of the ship is determined first. Afterward, the standard deviation is calculated by taking into account the variation in the height of the ship due to wave and tide. Finally, the normal distribution is generated. The detailed computations are presented in the following sub-sections.

4.2.1. Maximum height of the approach surface

The distances between the runway threshold and lane 1, lane 2 and lane 3 are measured to calculate the maximum height of the approach surface which is assumed as the maximum height of the ship. The distance from each individual lane to the runway threshold can be seen in Fig. 7.

After obtaining the distance, the maximum height of the approach surface is computed using the dimension and slope of the approach surface in Table 1. Fig. 8 demonstrates the way how we calculate the maximum height of the approach surface. In Fig. 8 we denote DA, EB, and FC respectively as the maximum height of the approach surface with respect to lane 1, lane 2 and lane 3. We therefore have $\frac{\text{DA}}{\text{AO}} = \frac{\text{EB}}{\text{BO}} = \frac{\text{FC}}{\text{CO}}$. From Table 1 we know that the distance from threshold is 60m. Thus, we have $\text{AO} = 2220 - 60 = 2160\text{m}$, $\text{BO} = 2440 - 60 = 2380\text{m}$, and $\text{CO} = 2610 - 60 = 2550\text{m}$. From Table 1 we also know that the slope is 2% for aircraft with aerodrome reference code number 3/4 performing a landing approach on the precision approach CAT I/II runway. As a consequence, we have $\text{DA} = \text{AO} \times 2\% = 43.2\text{m}$, $\text{EB} = \text{BO} \times 2\% = 47.6\text{m}$, and $\text{FC} = \text{CO} \times 2\% = 51\text{m}$.

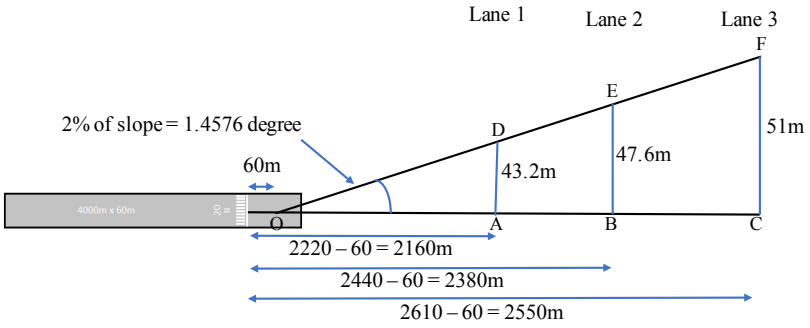

Figure 8: Computation method to find the maximum approach height for Code number 3/4 performing a landing approach on the precision approach CAT I/II runway.

The maximum height of the approach surface is assumed to be the mean height of the ship in Singapore Strait so as to ensure the maximum height limit is used in our research. The mean height of the ship for code number 3/4 in lane 2 will be used to derive the normal distribution. The mean height of the ship in lane 1 and lane 3 will be use for comparison in the next section.

4.2.2. Variation in height of ship

Ships moving along the Singapore Strait encounter tides and waves which affect the maximum height of the ship. Thus, it is important to account for additional height due to waves and tides. The maximum height of tides for the month of February 2019 is 3.4m [37]. The maximum height of tides on each day in February is shown in Fig. 9.

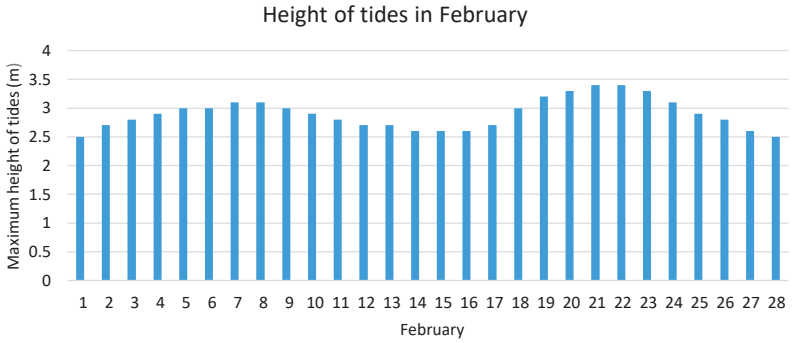

Figure 9: Maximum height of tides in February, 2019 [37].

The maximum height of wave is estimated to be 0.4m [38]. Therefore, a variation of 3.8m for the height of the ship is taken into consideration during the developing of algorithm to generate the normal distribution of the ship's height.

4.2.3. Computing standard deviation of ship's height

The mean height of ships is 47.6m and the maximum height of ship is equal to 47.6 + 3.8 = 51.4m. To find the standard deviation to generate a normal distribution, the study of normal distribution is required. Fig. 10(a) shows the empirical rule for the normal distribution.

Fig. 10(a), indicates that, 99.7% of the data fall within 3 standard deviation from the mean. Therefore, to determine the standard deviation of the ship, the maximum height of the tides and wave can be used to estimate the standard deviation. Firstly, 3.8m is taken to be equal to 3 standard deviation for which the standard deviation is equal to 1.2667. An algorithm is developed to check the maximum height of ship based on the mean of 47.6 and standard deviation of 1.2667 for 100,000 sample followed by plotting of the normal distribution of the ship. This algorithm requires the use of the external Python library NumPy to generate data to form a normal distribution and the library Matplotlib to display the normal distribution. The maximum height of the ship obtained by the standard deviation is 53m which has a big difference from the original maximum height of ship which is 51.4m. Therefore, instead of using 3 standard deviation from

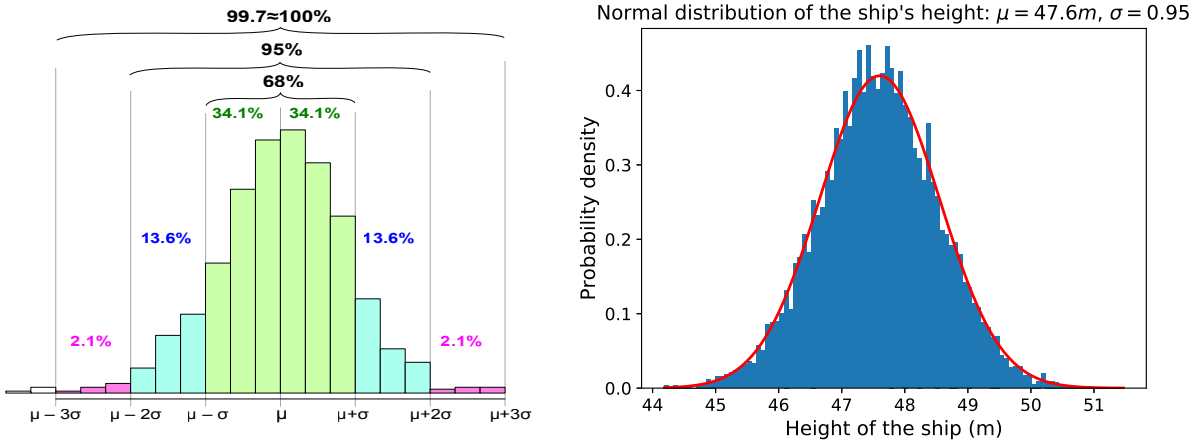

(a) (b)

Figure 10: Normal distributions. (a) The empirical rule for the normal distribution [39] and (b) the normal distribution of the ship's height.

the mean, 4 standard deviation from the mean is used. The standard deviation used is 3.8 divided by 4 which equals 0.95. The maximum height of the ship obtained by the standard deviation is 51.5m which is close to the original maximum height of the ship. Therefore, a mean of value 47.6 and standard deviation of 0.95 are used in the algorithm to determine the collision risk between a ship and an aircraft. Fig. 10(b) displays the normal distribution of the ship's height with a mean of 47.6m and standard deviation of 0.95 plot by using histogram as indicated in blue colour and a best fit line of the histogram as indicated in red colour.

4.3. Computing Normal Distribution of the Altitude of the Aircraft

The aircraft landing trajectory data is obtained from the ADS-B data purchased from FlightAware. It consists of 50 samples of different altitudes that range from 69.76m to 774.7m, and for each altitude it has its latitude, and its three upper and lower standard deviations from the mean. After organizing the original data, the standard deviation for each respective altitude can be obtained. From the 50 samples of different altitudes, interpolation is used to obtain the required altitude and its standard deviation. The data can be found in the Appendix. The required altitude is based on the latitude of where the lane 2 in the Singapore Strait start. The latitude of the lane 2 starting point is obtained from Google Map and interpolation is used to get the corresponding altitude and standard deviation. Instead of using the latitude of lane 2 in the middle, the latitude of lane 2 starting point is used due to better collision risk approximation in the final algorithm. The start of lane 2 defined as the lane in the middle of lane 1 and lane 2. Based on Fig. 7, the start of lane 2 is calculated as 2330m from the runway threshold and the corresponding latitude can be obtained.

Table 2: Mean altitude and its standard deviation for aircraft above lane 2 starting point.

	Point 1	Point 2	Lane 2 starting point
Latitude (°)	103.99612245	103.99714286	103.997076
Altitude (m)	154.7815	169.0436174	168.1091292
StdDevAlt	21.74806848	21.6881532	21.69207901

The latitude of the lane 2 starting point is 103.997076° and it is used to interpolate the corresponding altitude and its standard deviation based on the aircraft landing trajectory data. The two points (Point 1 (T7) and Point 2 (T8)) used for interpolation can be found in the Appendix and the altitude and its standard deviation of the lane 2 starting point is found to be 168.11m and 21.69 rounded off to 2 decimal points respectively. Table 2 shows the points used for interpolation and the mean and standard deviation of lane 2 starting point.

Fig. 11 displays the normal distribution of the aircraft altitude with a mean of 168.11m and standard deviation of 21.69 plot by using histogram as indicated in orange colour and a best fit line of the histogram as indicated in red colour.

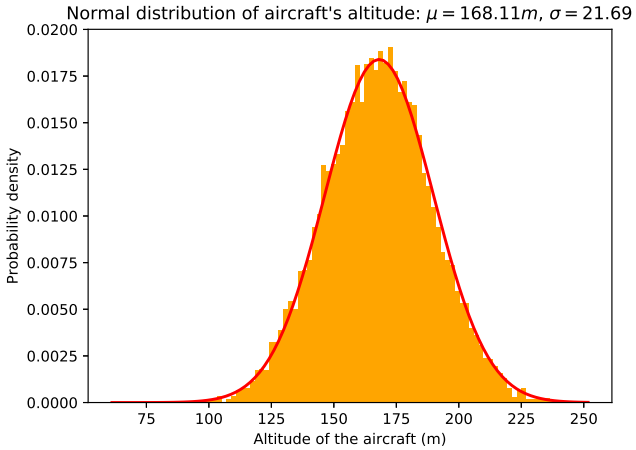

Figure 11: Normal distribution of the aircraft's altitude.

4.4. Determining the Collision Risk in the Approach Segment

Collision occurs when the normal distributions of ship and aircraft intersect each other. This occurs when the maximum value of the ship's height normal distribution is higher than the minimum value of the aircraft's altitude normal distribution. Fig. 12 displays the normal distribution of the ship's height with a mean of 47.6m and standard deviation of 0.95 together with the aircraft's altitude with a mean of 168.11m and standard deviation of 21.69.

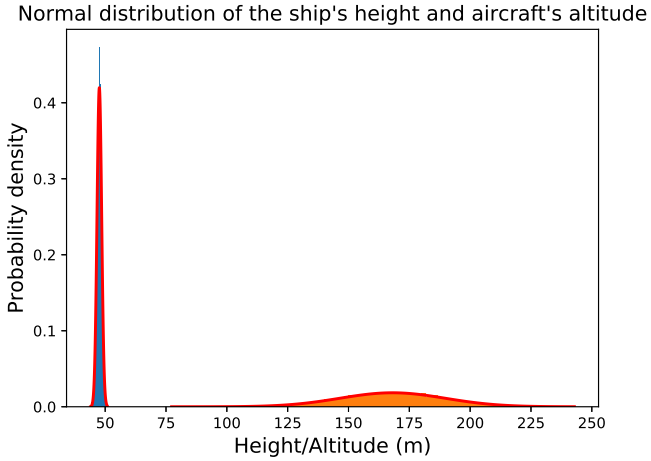

Figure 12: Normal distribution of ship's height and aircraft's altitude to determine the collision risk.

By using the data and information of the normal distribution of the ship's height and aircraft's altitude, the collision risk can be determined. When the differences between the aircraft minimum height of the aircraft landing trajectory normal distribution and the ship maximum height of the ship's height normal distribution is less than 0, it indicates that collision occurs. To find the collision probability, a function is created to loop the process of determining collision for 100,000 times. The collision risk is then quantified as the number of times collision occurs divided by 100,000.

4.5. Determine the Collision Risk as the Runway Threshold Reduce

When the runway threshold is shifted forward, the altitude of the aircraft will be reduced accordingly as the landing slope of the aircraft remains the same. Therefore, the further the runway threshold is shifted

forward, the lower the altitude of the aircraft at the same latitude. The landing slope is first initialized to be $tan^{-1}\frac{Alt_L}{Dist_L}$ which is calculated to be 4.13° for lane 2 where Alt_L is defined as the altitude of aircraft at a specific lane and $Dist_L$ is defined as the distance from the runway threshold to a specific lane. Using the distance between the runway threshold and the starting point of lane 2 which is 2330m as obtained from Fig. 7 and altitude of aircraft at lane 2 which is 168.11m as obtained from Table 2, the landing slope is computed as follow: $Landingslope = tan^{-1}\frac{168.11}{2330} = 4.13°$. Assuming that the landing slope remain the same when the runway threshold is shifted forward, in this case we shifted the runway threshold by 60m, the altitude of the aircraft is computed as follow: $Altitudeofaircraft = (2330 - 60) \times tan(4.13°)$. This is illustrated in Fig. 13.

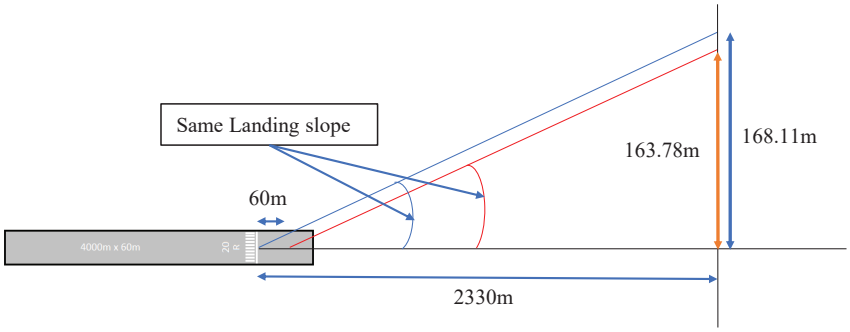

Figure 13: Reduction in the altitude of the aircraft based on the length of runway threshold shift.

Based on the idea to determine the collision risk between the ship and aircraft in the approach segment as mentioned previously and accounting for the collision risk as the runway threshold reduce, Algorithm 1 was developed to determine the collision risk between the aircraft and the ship in relation to the length of runway threshold shifted.

Algorithm 1 Determine the collision risk between the aircraft and the ship in relation to the length of runway threshold shifted.

1. Define the landing slope of the aircraft $LS = tan^{-1}\frac{Alt_L}{Dist_L}$, where Alt_L is the altitude of aircraft at a specific lane and $Dist_L$ is the distance from the runway threshold to a specific lane;
2. Define $Threshold\_shift = [\ ]$, $Altitude = [\ ]$, and $CR = [\ ]$;
3. Set $Threshold\_shift = 0 : 10 : 300$;
4. $\forall d \in Threshold\_shift$, $Altitude = [Altitude,\ (Dist_L - d) * tan(LS)]$;
5. **For** t in $Altitude$, **do**
   (a) Initialize $x = 0$ and $y = 0$;
   (b) **While** $x < 100000$, **do**
      i. $ship\_height = NormalDistribution(\mu_s, \sigma_s, 10000)$;
      ii. $ship\_highest = max(ship\_height)$;
      iii. $aircraft\_altitude = NormalDistribution(\mu_a, \sigma_a, 10000)$;
      iv. $aircraft\_lowest = min(aircraft\_altitude)$;
      v. $Diff = aircraft\_lowest - ship\_highest$; //indicate collision
      vi. If $Diff \leq 0$, then $y = y + 1$;
      vii. $x = x + 1$;
   (c) **End While**
   (d) $CR = [CR,\ y/100000]$. //collision risk calculation
6. **End**

Algorithm 1 will take account up to 300m of the runway threshold shift with an interval of 10m. The corresponding altitude of the aircraft for each of the interval is calculated using the fixed initialized landing slope of 4.13° and the length of threshold shifted. The collision risk at every interval of 10m of runway threshold shift is determined.

5. Experimental Results

5.1. Collision Risk for Shipping Lane 2

After applying the collision risk calculation method to Lane 2 of the Singapore Strait, the results are reported in the form of a scatter plot. Fig. 14 displays scatter plot in which the variations of the collision risk and the altitude of the aircraft above Lane 2 are shown with respect to the variation of the shifted runway threshold.

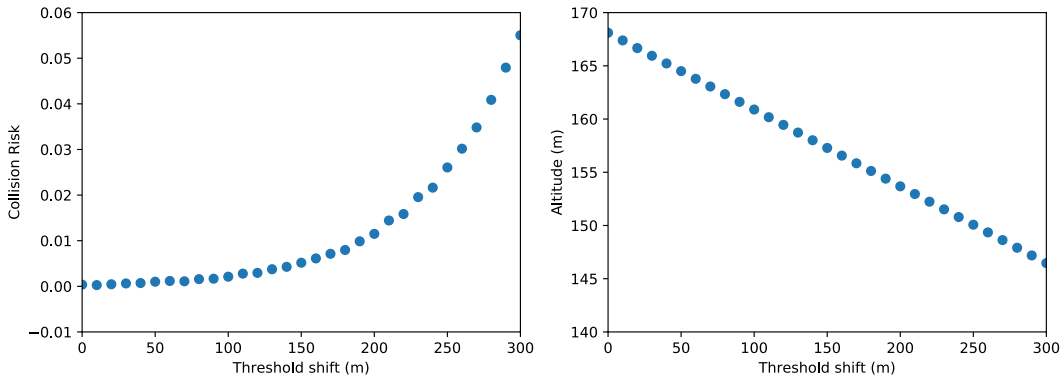

Figure 14: Scatter plot of the collision risk vs length of runway threshold shifted on the left and the altitude vs length of runway threshold shifted on the right for Lane 2.

From Fig. 14, the collision risk varies from 0 to 0.055 with respect to the threshold shift and the altitude of the aircraft decreases linearly from 168.11m to 146.46m when the length of threshold shift increases from 0m to 300m. It can be observed that the collision risk increases exponentially when the length of threshold shifted is more than 150m.

5.2. Collision Risk for Shipping Lanes 1 and 3

In the above subsection, the collision risk between the ship and aircraft is determined for the shipping lane 2 in the Singapore Strait. In order to ensure that the collision risk obtained for shipping lane 2 is accurate, the collision risk for the other two shipping lanes in Singapore Strait are required to be determined. Using Algorithm 1, the collision risk for lanes 1 and 3 can be determined but the variables used for computation are different. The latitude of the aircraft is based on the shipping lane and therefore the altitude of the aircraft will change accordingly based on the fixed initialized landing slope on each lane which is also different. The mean and standard deviation of the ship's height and aircraft's altitude will change accordingly based on the shipping lane. The latitude of lane 1 is taken at the middle due to uncertainty of the start of lane 1, while the latitude of lane 3 is taken from the starting point of lane 3. The latitudes of the lanes are obtained from the google maps as shown in Fig. 7.

The latitudes of the lane 1 middle point and lane 3 starting point are 103.996640° and 103.997751° respectively. Following which, they are used to interpolate the corresponding altitude and its standard deviation based on the aircraft landing trajectory data. The two set of points (Point 1 (T7) and Point 2 (T8), Point 1 (T8) and Point 2 (T9)) used for interpolation are reported in the Appendix for lane 1 and 3 respectively, and the altitudes and standard deviations of lane 1 middle point and lane 3 starting points are interpolated to be 162.02m, 21.72 and 177.56m, 21.66, rounded off to 2 decimal point respectively. Tables 3 shows the points that is used for interpolation and the acquired mean and standard deviation for lane 1 middle point and lane 3 starting point.

After obtaining the altitude of aircraft at lane 1 and 3, the landing slope can be computed. The landing slopes of lane 1, 2 and 3 are calculated to be 4.17°, 4.12° and 4.02° respectively. Referring to Fig. 8, the maximum allowable heights of the ship for lane 1 and lane 3 are 43.2m and 51m, respectively. Following the

Table 3: Mean altitudes and their standard deviations for aircraft above lane 1 middle point and lane 3 starting point

Lane	Lane 1			Lane 3		
Point	Point 1	Point 2	Lane 1 middle point	Point 1	Point 2	Lane 3 starting point
Latitude (°)	103.99612	103.99714	103.99664	103.99714	103.99816	103.99775
Altitude (m)	154.78150	169.04361	162.01525	169.04362	183.32902	177.55738
StdDevAlt	21.748068	21.68815	21.71768	21.68815	21.63838	21.65849

previous assumption, the maximum allowable height is assumed to be the mean of the ship for generating the normal distribution. The standard deviations of the ship's height normal distribution of lane 1 and lane 3 are the same as that of lane 2 which is 0.95 as the standard deviation is obtained from the height variation due to tides and waves which are the same for all the lanes in Singapore Strait. After obtaining the required data, the collision risk can now be determined using Algorithm 1.

After applying the collision risk calculation method to lanes 1 and 3 of the Singapore Strait, the results of the collision risk are obtained in form of scatter plot. Fig. 15 displays the scatter plots in which the variations of the collision risk and the altitude of the aircraft above lanes 1 and 3 are shown with respect to the variation of the shifted runway threshold.

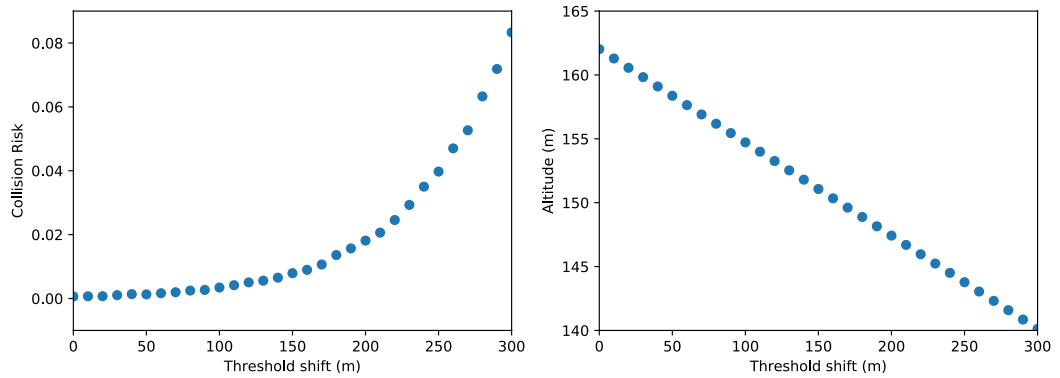

(a) Lane 1

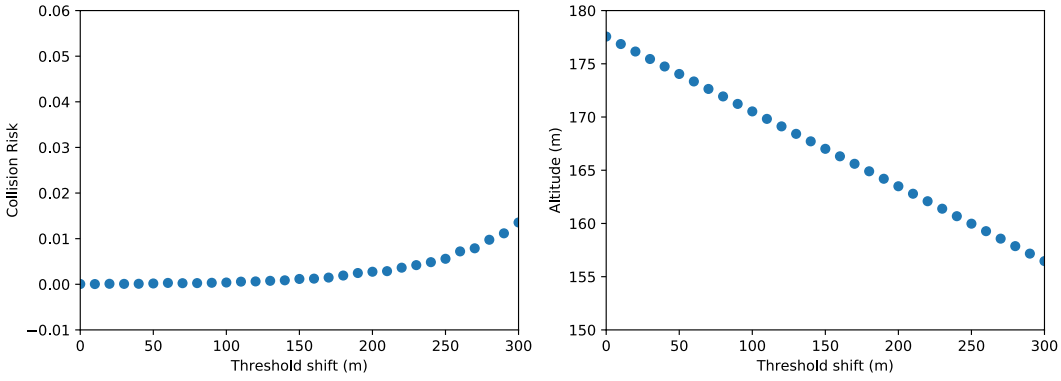

(b) Lane 3

Figure 15: Scatter plots of the collision risk vs length of runway threshold shifted on the left and the altitude vs length of runway threshold shifted on the right for lanes 1 and 3.

As can be seen from Fig. 15(a), the collision risk varies from 0 to 0.08 with respect to the threshold shift. The altitude of the aircraft decreases linearly from 162.02m to 140.13m when the length of threshold shift increases from 0m to 300m. It can be observed that the collision risk increases exponentially if the length of threshold shifted is more than 150m. The similar phenomena also can be discovered from what are shown in Fig. 15(b). From Fig. 15(b) we see that the collision risk does not increase exponentially when the length of threshold shifted is more than 150m. This is because that lane 3 is relatively far away from the runway and its impacts on the collision risk are therefore relatively smaller than that of lanes 1 and 2.

5.3. Discussions

Based on the above results, it is certain that the collision risk increases as the length of the runway threshold shifted increases. This is due to the decrease in aircraft's altitude as the length of runway threshold shifted increases resulting in greater proximity of the aircraft to the shipping lanes. Furthermore, it can be observed that the collision risk increases more rapidly when the length of threshold shift passes a critical point. The critical point for lane 1 and lane 2 is 100m but for lane 3 is 200m. The reason for lane 3 having a higher critical point than lanes 1 and 2 is due to the increase in vertical separation of the ship and aircraft. When the distance between the shipping lane and runway threshold increase, the separation space between the ship and aircraft also increases. Fig. 16 presents the relationship between the shifted runway threshold and the vertical separation between the ship and aircraft. Based on the differences of the height of the ship (refer to Fig. 8) and the altitude of aircraft (assuming a constant landing slope of 4.02°) which is known as the vertical separation. We can observe that, as the vertical separation distance increase, the collision risk will decrease.

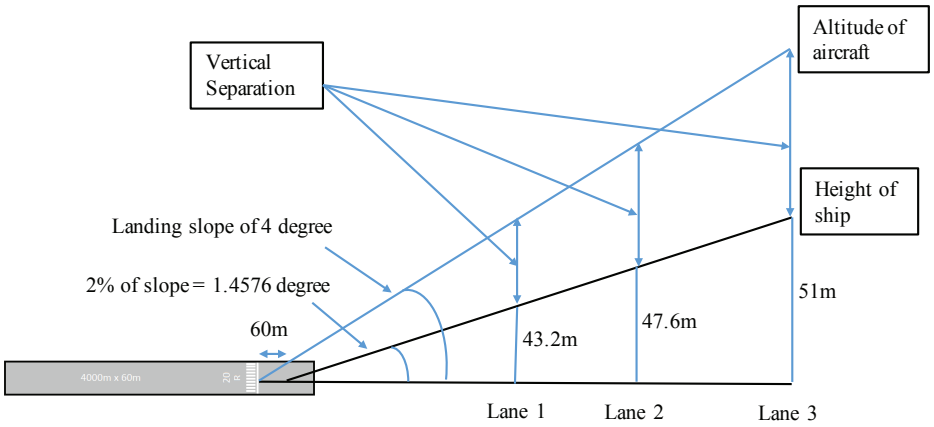

Figure 16: Vertical separation between the ship and aircraft increase for lane that is further from the runway threshold.

For all the three studied lanes, we can see from Figs. 14 and 15 that the collision risk with respect to lane 1 is the highest, while the values of the collision risk increase exponentially when the shifted runway threshold surpasses 100m. We therefore suggest that the runway threshold of runway 20R of Changi Airport can be reduced by 100m.

6. Concluding Remarks

The constructions of airports may suffer from obstruction constraints. When an aerodrome is surrounded by obstructions, a displaced threshold is assigned to the runway to maintain the safety standard for departures and arrivals of the flights. Note that the displaced thresholds for the runways of some airports were determined in a very conservative way. Such conservative thresholds decrease the LDA of the runways impacting the runway capacity.

This paper provided a new perspective for dynamic runway threshold management by reducing the runway threshold as and when required. To do so, a data-driven collision risk method, that makes full use of the flight approach path and obstacle surface profile, was suggested. To validate the feasibility the model is developed and applied to Singapore Changi Airport, which suffers from long displaced runway threshold due to the ship movements in Singapore Strait Channel. The proposed method was applied to three different shipping lanes in Singapore Strait to determine the collision risk between the aircraft on approach path and the ships in their respective lanes with respect to different distances of runway threshold. The results indicated that the three lanes have a similar trends of collision risk increasing as the length of runway threshold shifted increases. The collision risk was observed to be lower for the shipping lane that is further from the runway threshold (lane 3) as compared to the nearer lane (lane 1 and 2) due to the differences in vertical separation. The results of lane 1 were used for further analysis to determine the length of runway threshold that can be shifted as using the lane with higher collision risk will have a higher safety margin. It was suggested that a maximum length of runway threshold that can be reduced is 100m.

For the case study, there are few limitations in determining the collision risk between the ship and the aircraft. The original landing trajectories were obtained for a specific category of aircraft, which shows a high standard deviation in its vertical profile. High standard deviation of an aircraft can result in higher collision risk. Lastly, the safety distance between the ship and aircraft had not been considered in this project although the maximum limits of the ship and aircraft was used to determine the collision risk.

Although there exist several well-known collision risk calculation methods in the literature [40–43], the one developed in this work is much simpler as it only considers the flight approach path and the obstacles surface profile without taking into account the Navigational error of Instrument Landing System (ILS), Required Navigation Performance (RNP)/RNAV procedures and meteorological data. In our future work, we will investigate the impact of different collision risk calculation methods on the reduced runway threshold. Although the case study is only carried out for Singapore Changi Airport, the generalization of the framework of the proposed method to other airports that are subject to obstruction constraints is apparent. For future planning of airports, that are to be built on reclaimed land or nearby the straits, where there are possible ship movement obstructing the surrounding airspace, this study can be used to assist with the assignment of displaced threshold distance for given runways.

Acknowledgements

This research is partially supported by SUG Grant 04INS000398C160 from the School of Mechanical and Aerospace Engineering, NTU Singapore.

References

[1] M. C. Gelhausen, P. Berster, D. Wilken, Do airport capacity constraints have a serious impact on the future development of air traffic?, Journal of Air Transport Management 28 (2013) 3–13.

[2] S. Dunn, S. M. Wilkinson, Increasing the resilience of air traffic networks using a network graph theory approach, Transportation Research Part E: Logistics and Transportation Review 90 (2016) 39–50. Risk Management of Logistics Systems.

[3] S. Wilke, A. Majumdar, W. Y. Ochieng, Airport surface operations: A holistic framework for operations modeling and risk management, Safety Science 63 (2014) 18–33.

[4] IATA, IATA forecast predicts 8.2 billion air travelers in 2037, https://www.iata.org/pressroom/pr/pages/2018-10-24-02.aspx, 2018.

[5] C. Barnhart, D. Fearing, A. Odoni, V. Vaze, Demand and capacity management in air transportation, EURO Journal on Transportation and Logistics 1 (2012) 135–155.

[6] D. Bertsimas, S. S. Patterson, The air traffic flow management problem with enroute capacities, Operations Research 46 (1998) 406–422.

[7] S. H. Stroeve, H. A. Blom, G. Bakker, Systemic accident risk assessment in air traffic by monte carlo simulation, Safety Science 47 (2009) 238–249.

[8] Q. Yang, J. Tian, T. Zhao, Safety is an emergent property: Illustrating functional resonance in air traffic management with formal verification, Safety Science 93 (2017) 162–177.

[9] K. G. Zografos, M. A. Madas, K. N. Androutsopoulos, Increasing airport capacity utilisation through optimum slot scheduling: review of current developments and identification of future needs, Journal of Scheduling 20 (2017) 3–24.

[10] A.-M. Teperi, A. Leppänen, Managers' conceptions regarding human factors in air traffic management and in airport operations, Safety Science 49 (2011) 438–449.

[11] B. Vaaben, J. Larsen, Mitigation of airspace congestion impact on airline networks, Journal of Air Transport Management 47 (2015) 54–65.

[12] J. Rakas, A. Bauranov, B. Messika, Failures of critical systems at airports: Impact on aircraft operations and safety, Safety Science 110 (2018) 141–157.

[13] A. Lieder, R. Stolletz, Scheduling aircraft take-offs and landings on interdependent and heterogeneous runways, Transportation Research Part E: Logistics and Transportation Review 88 (2016) 167–188.

[14] J. A. Bennell, M. Mesgarpour, C. N. Potts, Airport runway scheduling, 4OR 9 (2011) 115.

[15] A. Kanafani, Operational procedures to increase runway capacity, Journal of Transportation Engineering 109 (1983) 414–424.

[16] M. Janic, Modeling effects of different air traffic control operational procedures, separation rules, and service disciplines on runway landing capacity, Journal of Advanced Transportation 48 (2014) 556–574.

[17] D. M. Lohr, Gary W.; Williams, Current Practices in Runway Configuration Management (RCM) and Arrival/Departure Runway Balancing (ADRB), Technical Report NASA/TM-2008-215557, L-19505, LF99-7407, NASA Langley Research Center, Hampton, VA, United States, 2008.

[18] M. D. Christopher Weld, R. Kincaid, A runway configuration management model with marginally decreasing transition capacities, Advances in Operations Research 2010 (2010) 1–22.

[19] D. Bertsimas, M. Frankovich, A. Odoni, Optimal selection of airport runway configurations, Operations Research 59 (2011) 1407–1419.

[20] T. Kolos-Lakatos, The influence of runway occupancy time and wake vortex separation requirements on runway throughput, Ph.D. thesis, Massachusetts Institute of Technology, 2013.

[21] G. Lohr, S. Brown, H. Stough, S. Atkins, S. Eisenhawer, D. Long, System oriented runway management: A research update, in: Ninth USA/EUROPE Air Traffic Management Research and Development Seminar, Berlin; Germany.

[22] F. Farhadi, A. Ghoniem, M. Al-Salem, Runway capacity management–an empirical study with application to doha international airport, Transportation Research Part E: Logistics and Transportation Review 68 (2014) 53–63.

[23] E. P. Gilbo, Optimizing airport capacity utilization in air traffic flow management subject to constraints at arrival and departure fixes, IEEE Transactions on Control Systems Technology 5 (1997) 490–503.

[24] S. J. Heblij, R. A. A. Wijnen, Development of a runway allocation optimisation model for airport strategic planning, Transportation Planning and Technology 31 (2008) 201–214.

[25] G. Wei, J. Siyuan, Simulation study on closely spaced parallel runway analysis using SIMMOD plus, in: 2010 International Conference on Intelligent Computation Technology and Automation, volume 3, Changsha, China, pp. 344–347.

[26] Y.-H. Liu, A genetic local search algorithm with a threshold accepting mechanism for solving the runway dependent aircraft landing problem, Optimization Letters 5 (2011) 229–245.

[27] S. S. A. Aiyar, The case for offshore airports, https://www.cato.org/publications/commentary/case-offshore-airports, 2003.

[28] H.-K. Yan, N. Wang, L. Wei, Q. Fu, Comparing aircraft noise pollution and cost-risk effects of inland and offshore airports: The case of dalian international airport, dalian, china, Transportation Research Part D: Transport and Environment 24 (2013) 37–43.

[29] I. Kirkland, R. Caves, I. Humphreys, D. Pitfield, An improved methodology for assessing risk in aircraft operations at airports, applied to runway overruns, Safety Science 42 (2004) 891–905.

[30] R. M. A. Valdés, F. G. Comendador, L. M. Gordún, F. J. S. Nieto, The development of probabilistic models to estimate accident risk (due to runway overrun and landing undershoot) applicable to the design and construction of runway safety areas, Safety Science 49 (2011) 633–650.

[31] ICAO, Volume 1 Aerodrome Design and Operation, 4th Edition, 2004.

[32] Department of Statistic, Civil aircraft arrivals, departures, passengers and mail, changi airport, annual, https://www.tablebuilder.singstat.gov.sg/publicfacing/displaychart.action, (Accessed Nov 06, 2019).

[33] Singapore Infopedia, Changi Airport, http://eresources.nlb.gov.sg/infopedia/articles/sip_574_2004-12-23.html, (Accessed Nov 06, 2019).

[34] H. S. L. Fan, Effect of local operational constraints on runway capacity - a case study, Journal of Advanced Transportation 26 (1992) 169–184.

[35] CAAS, AIP Singapore, https://www.caas.gov.sg/docs/default-source/pdf/aip-10oct19.pdf, (Accessed Nov 06, 2019).

[36] FAA, Section 3. Airport Marking Aids and Signs, https://www.faa.gov/air_traffic/publications/atpubs/aim_html/chap2_section_3.html, (Accessed Nov 06, 2019).

[37] Meteorological Service Singapore, Astronomical data and tides, http://www.weather.gov.sg/weather-astronomical-and-tidal-information-monthly-data, (Accessed Nov 06, 2019).

[38] Windfinder, Wind, waves & weather forecast (Singapore Changi Airport), https://www.windfinder.com/forecast/singapore_changi, (Accessed Nov 06, 2019).

[39] D. Kernler, A visual representation of the Empirical (68-95-99.7) Rule based on the normal distribution, https://commons.wikimedia.org/wiki/File:Empirical_Rule.PNG#/media/File:Empirical_rule_histogram.svg, 2014.

[40] C. Thiel, H. Fricke, Collision risk on final approach–a radar-data based evaluation method to assess safety, in: Proceedings of the International Conference on Research in Air Transportation (ICRAT). Budapest, Hungary.

[41] A. Silva, A. G. de Barros, Quantitative risk evaluation of obstacle limitation surfaces for final approaches at airports, Journal of Aviation Technology and Engineering 5 (2016) 5.

[42] H. Fricke, S. Förster, M. Vogel, Using agent-based modeling to determine collision risk in complex tma environments: the turn-onto-ils-final safety case, Aeron Aero Open Access J 2 (2018) 155–164.

[43] H. Fricke, C. Thiel, et al., A methodology to assess the safety of aircraft operations when aerodrome obstacle standards cannot be met, Open Journal of Applied Sciences 5 (2015) 62.

Appendix

Table 4: Aircraft landing trajectories obtain from ADS-B data.

ID	MeanAlt (m)	Latitude (°)	StdDevAlt	ID	MeanAlt (m)	Latitude (°)	StdDevAlt
T1	69.764837230	103.99	22.38772077	T26	428.63997923	104.01551020	21.49908556
T2	83.862520520	103.99102041	22.24142751	T27	443.14754019	104.01653061	21.49993505
T3	97.990388750	103.99204082	22.11274429	T28	457.65614672	104.01755102	21.50005472
T4	112.14733142	103.99306122	22.00035019	T29	472.16479845	104.01857143	21.49945598
T5	126.33224215	103.99408163	21.90294827	T30	486.67202246	104.01959184	21.49821091
T6	140.54401371	103.99510204	21.81926750	T31	501.17667912	104.02061224	21.49644655
T7	154.78156033	103.99612245	21.74806848	T32	515.67776559	104.02163265	21.49434593
T8	169.04361754	103.99714286	21.68815320	T33	530.17389530	104.02265306	21.49214847
T9	183.32902431	103.99816327	21.63837660	T34	544.66392937	104.02367347	21.49016024
T10	197.63673636	103.99918367	21.59762711	T35	559.14667588	104.02469388	21.48873176
T11	211.96560071	104.00020408	21.56486194	T36	573.62081771	104.02571429	21.48828034
T12	226.31448062	104.00122449	21.53908405	T37	588.08545103	104.02673469	21.48928797
T13	240.68209043	104.00224490	21.51935897	T38	602.53906706	104.02775510	21.49228631
T14	255.06743619	104.00326531	21.50481203	T39	616.98055668	104.02877551	21.49787284
T15	269.46922126	104.00428571	21.49463232	T40	631.40879524	104.02979592	21.50671116
T16	283.88624154	104.00530612	21.48806447	T41	645.82251384	104.03081633	21.51951643
T17	298.31752024	104.00632653	21.48441374	T42	660.22056249	104.03183673	21.53707672
T18	312.76159767	104.00734694	21.48305580	T43	674.60171649	104.03285714	21.56022985
T19	327.21764546	104.00836735	21.48342427	T44	688.96479780	104.03387755	21.58987868
T20	341.68423123	104.00938776	21.48500329	T45	703.30854330	104.03489796	21.62698926
T21	356.16018784	104.01040816	21.48735190	T46	717.63198409	104.03591837	21.67257715
T22	370.64439197	104.01142857	21.49008339	T47	731.93359662	104.03693878	21.72771856
T23	385.13568576	104.01244898	21.49286352	T48	746.21245624	104.03795918	21.79353937
T24	399.63284041	104.01346939	21.49542272	T49	760.46723306	104.03897959	21.87121297
T25	414.13466186	104.01448980	21.49754676	T50	774.69688316	104.04	21.96195057